INTERNATIONAL JOURNAL OF HYDROGEN ENERGY 45 (2020) 891–903

Available online at www.sciencedirect.com

ScienceDirect

journal homepage: www.elsevier.com/locate/he

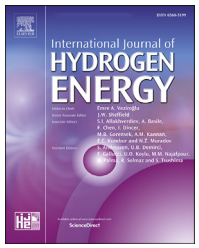

Interline fuel cell (I-FC) system with dual-functional control capability

Mustafa İnci

İskenderun Technical University, Department of Mechatronics Engineering, İskenderun, Hatay, Turkey

HIGHLIGHTS

- A novel concept called I-FC system is presented in this work.
- In I-FC concept, a single fuel cell system is connected to multi-feeders through separate inverters.
- A dual functional controller based on αβ-dq transform is developed and performed in the grid inverters.
- The system achieves to share active powers and attenuate the current harmonics, simultaneously.

ARTICLE INFO

Article history:
Received 25 July 2019
Received in revised form
29 September 2019
Accepted 16 October 2019
Available online 11 November 2019

Keywords:
Interline fuel cell
Grid inverters
Interfacing
Power sharing
Current harmonics

ABSTRACT

In this paper, a new system concept is presented for the grid connection of fuel cells. In conventional grid-connected systems, fuel cells ensure the generated power into a single electrical feeder and control the electrical-line through interfacing elements. In the proposed system, interline fuel cell (I-FC) system shares a common dc-dc converter tied fuel cell at the base of inverters and eliminates the additional fuel cell & dc-dc converter in a multi-feeder system. For this purpose, a fuel cell system is connected to multi-feeders through separate inverters, thereby sharing electrical power into the feeders and attenuating the harmonics at grid-side currents. In this direction, the proposed system presents an economical way for the mitigation of electrical problems for multi-feeders. In order to achieve the functional capabilities of I-FC system, dual-functional control is separately applied in the grid inverters. In the testing stage of I-FC, nonlinear loads in feeder I & feeder II create 31.29% and 27.61% total harmonic distortion (THD) at grid-side currents, respectively. With I-FC, the THD values are reduced to approximately 3% values in both feeders after the harmonic elimination capability. Also, I-FC allocates the active power to both feeders, and reduces the electrical power demand from the utility-grids. The evaluation results verify that I-FC system accomplishes the good performance to control power-sharing and attenuate the current harmonics at grid-side.

Introduction

The major reduction in fossil fuels and the environmental effects such as harmful gas emissions, natural events and the community health, play an important role to be interested in renewable energy generation systems that are environmentally friendly and clean. In renewable energy technologies, the role of fuel cell systems in a power plant is permanently increasing due to the energy demand. Because, the fuel cells

E-mail address: mustafa.inci@iste.edu.tr.
https://doi.org/10.1016/j.ijhydene.2019.10.122

Nomenclature

A	Tafel slope
AC	Alternating current
D	Duty cycle
DC	Direct current
F	Faraday constant
FC	Fuel cell
FFT	Fast Fourier Transform
h	Hysteresis band value
$I_{error,n}$	Reference value used in switching process
$I_{p-error,n}$	Reference value of power component in I-FC control
$I_{har,n}$	Reference value of harmonic component in I-FC control
IEEE	Institute of Electrical and Electronics Engineers
I-FC	Interline fuel cell
N	Cell number in fuel cell
$P_{ref,n}$	Active power reference value for a feeder
$P_{sys,n}$	Active power supplied from fuel cell for a feeder
P_{total}	Total active power supplied from fuel cell
PEMFC	Proton exchange membrane fuel cell
PI	Proportional integral
$Q_{ref,n}$	Reactive power reference value for a feeder
$Q_{sys,n}$	Reactive power supplied from fuel cell for a feeder
Q_{total}	Total reactive power supplied from fuel cell
R_c	Gas constant in fuel cell
T	Operating temperature of fuel cell
THD	Total harmonic distortion
V_{fc}	Fuel cell output voltage
V_{oc}	Open circuit voltage in fuel cell
V_{Ω}	Resistivity overvoltage in fuel cell
v_d	Absolute polarization overvoltage in fuel cell
V_{dc}	DC-link voltage
$V_{dc,ref}$	Reference value for dc-link voltage
z	Number of electrons moving in fuel cell

are very desirable owing to their excellent characteristics: low/zero emissions, simple implementation, high efficiency and modular design [1–3]. Additionally, these structures ensure a significant way to balance power flows and regulate voltage/frequency in comparison to the discontinuous power supply such as wind and solar energy [4]. In recent years, fuel cell systems are integrated with the different electrical systems, and one of the fastest developments is the connection with grids [5–7]. The connection of fuel cells and electrical grids is entitled as grid-connected fuel cell system. This connection of fuel cells with grids is executed to lessen the electrical power demand supplied from the conventional supplies. By this way, it is understandable that the electrical power generated through fuel cell systems can be consumed immediately in electrical applications and/or be sold to the distribution firms [8,9].

Fuel cell power generation structures are conventionally connected in a single-electrical feeder to support the electrical grid power. This connection minimizes the instantaneous variations and improves the system performance and safety [10,11]. However, the electrical conversion is essential to transform the electricity from dc power to ac power in the grid-connected fuel cells [7,12]. Therefore, fuel cells are integrated to utility-grids via electronic converter based interface elements. In the integration process, dc-ac conversion and the power flow management from fuel cells to the grids are normally achieved through the inverter components [13,14]. In the interfacing components of grid/fuel cell systems, dc/dc converter is an element and its main function is to regulate the input-side voltage at the inverter by keeping in the range of ±5% [15]. In this context, it is obvious that the principal function of fuel cells connected to the grids is provided through inverters. Therefore, the function of the inverter is to control the active power delivered from the fuel cell to the grids/loads. In addition, it controls the reactive power flow between the fuel cell and the main grid [16].

In conventional grid-connected systems, fuel cell energy generation units are connected to the single feeders in order to supply controlled power [17]. Among structures connected to single-feeder, the systems include a fuel cell, a dc-dc converter, an inverter, an output filter and isolation transformer connected to the electrical grids. The main function of conventional grid connected fuel cell systems is to supply only active power for local loads/grids [18–31]. In addition to power flow control capability, the grid-connected fuel cell systems are also performed for additional functions [32]. Among these studies, a significant number of studies not only control power flow but also deal with the compensation of power quality problems [33,34]. In the grid connected fuel cell systems. Current harmonics are the most hazardous problems, which are defined as distorted currents. At grid-side, these problems effect the current quality as the result of nonlinear loads. Also, current harmonics are distorted currents which [35]. In the grid connected fuel cell systems, total harmonic distortion (THD) at grid-currents should be smaller than 5% according to the defined IEEE 2014.519 standards [36]. In Refs. [12,26,37–41], current harmonics are analysed and compensated in order to prevent the negative influences in systems connected to single-feeder. In addition to current harmonic problems in the utility-grids, reactive power flow is discussed in Refs. [42,43]. Also, the studies in Refs. [15,44–46] are interested in voltage sag/swell that induce hydrogen pressure in fuel cells. The study in Ref. [47] presents a flexible control strategy with overcurrent limiting capability for fuel cell connected hybrid system. Also, a study is proposed to maximize power delivery capability for fuel cell tied hybrid system [48]. In Ref. [49], frequency problems are analysed in addition to power flow control capability. However, in almost all of the investigated studies, it is clear that the complete systems related to grid connected fuel cells are connected to single-line electrical grids through a single inverter system, as shown in Fig. 1. For this purpose, the current study presents a novel concept of interline fuel cell (I-FC) system in which two grid inverters in different feeders are connected to a common fuel cell energy generation unit. In the proposed concept, the grid inverters share a common dc-dc converter based fuel cell system in order to supply partial active powers for different feeders and achieve the simultaneous compensation current harmonics at both two feeders. In this context, it eliminates an additional fuel cell and dc-dc converter in order to compensate current harmonics at separate multi-feeders. By this way, the present study introduces a

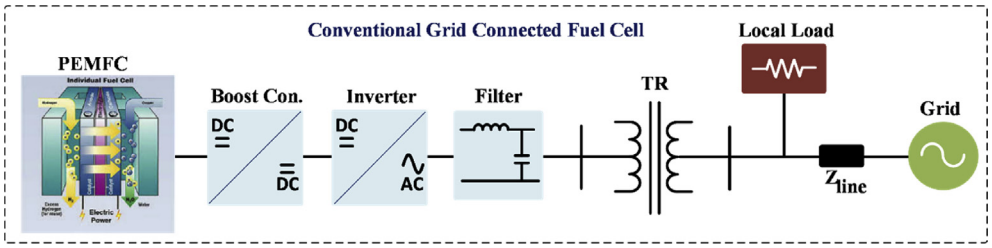

Fig. 1 – The single line diagram of a conventional grid-connected PEMFC system.

novel and economical approach for multiline current harmonic elimination in comparison with conventional systems connected to single-feeder. In the operational process of the proposed system, each inverter is operated in both power flow and harmonic attenuation modes.

In this paper, a single proton exchange membrane fuel cell (PEMFC) system with a dc-dc converter is designed to control two feeders by using separate inverters connected to single dc-dc converter based PEMFC. In the proposed topology, 19.3 kW grid-connected PEMFC system consisting of a Ballard Stack Modules-FCvelocity 9SSL is developed according to the operating principals of a PEMFC module. In the proposed system topology, the original contributions are given as:

- In I-FC system, PEMFC pattern applied in this paper is developed and validated according to the dynamic characteristics of the stack model.
- Grid-connected I-FC system is developed to supply shared active powers and attenuate the current harmonics by controlling two feeders, simultaneously.
- The system reduces the additional fuel cell/boost converter in comparison with a system connected to single-feeder. By this way, it is an economical way for multi-feeder system in order to provide current quality at grid-side.
- This paper also presents a dual-functional control scheme for I-FC system working in power supplying and current harmonics elimination in two different feeders.
- For the operation of grid inverters, αβ-dq transform based control method is developed for duel-functional control capability. For this purpose, the control algorithm is tested in two-feeders for two-functional capabilities: power flow control and current harmonic elimination.

This study is constructed as follows: the structural configuration of the grid-connected I-FC system is defined and

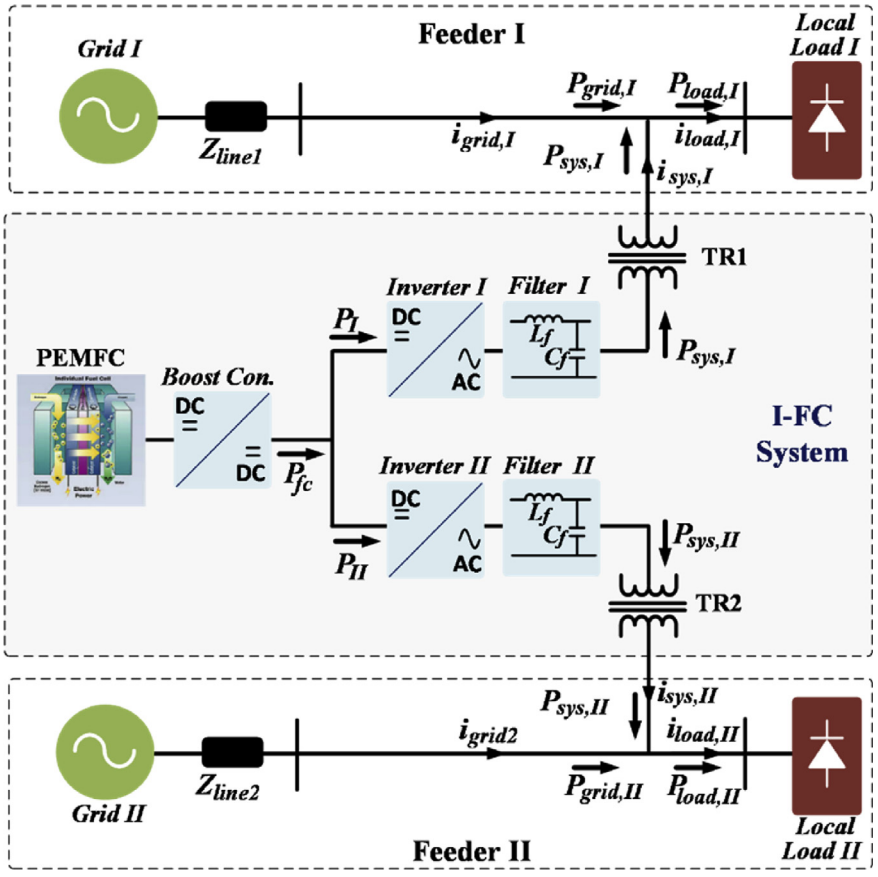

Fig. 2 – The proposed system: I-FC.

Table 1 – The design parameters of Ballard FCvelocity 9SSL.

Parameter	Value	Unit
Cell number	110	[–]
Voltage at 0 A and 1 A	[106.15,104.61]	[V,V]
Nominal operating point	[260,73.4]	[A,V]
Maximum operating point	[320,64]	[A,V]
PEMFC active region	285.8	[cm^2]
Anode capacity	0.014	[m^3]
Cathode capacity	0.00078	[m^3]
Stack capacity	0.014	[m^3]
H combustion	285.5	[kJ mol^{-1}]
Faraday constant (F)	96.485	[C mol^{-1}]
Thermal capacitance	17.9	[kJ C^{-1}]
Water heat capacity	4.184	[kJ kg^{-1} K^{-1}]
Universal gas constant	8.314	[J mol^{-1} K^{-1}]

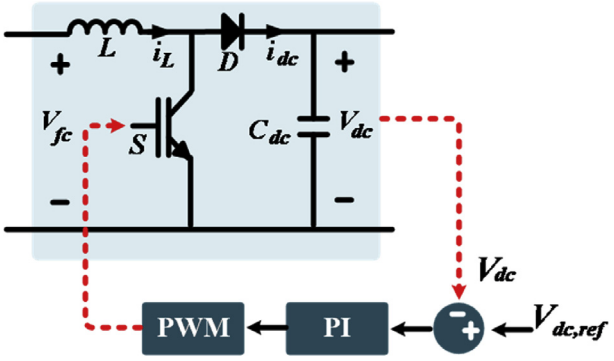

Fig. 3 – Dc-dc boost converter in I-FC system.

its arrangement procedure is introduced in Section I-FC System and design. In Section I-FC Control, the dual functional controller scheme of I-FC system is given in detail. The computer experiments are exhibited in Section Performance results in order to validate the effectiveness of I-FC system. In the last section, a conclusion is summarized in Section Conclusion.

I-FC system and design

Fig. 2 shows the power circuit scheme of the grid-connected I-FC system arranged in the proposed system. According to the circuit scheme, I-FC consists of a single PEMFC module, a single boost dc-dc converter, and grid-inverters with output filters in order to control the power flow and harmonic elimination at two separate feeders. The detailed information of I-FC system configuration will be introduced in subsections.

PEMFC

In power system applications, PEMFC is the most common fuel cell type which generates electrical power in dc-form [13]. For this purpose, the dynamic model of PEMFC used in I-FC system is presented in this section. The electrical characteristic behavior of PEMFC is given in Eqs. (1)–(4) [50]. Also, the operating voltage of fuel cell is computed as [26]:

$$V_{fc} = V_{oc} - V_{\Omega} - v_d \tag{1}$$

In which, V_{fc} is the instantaneous voltage at stack output, V_{oc} is defined as the open-circuit voltage, V_{Ω} is the resistivity overvoltage and v_d is the absolute polarization overvoltage (the function of oxygen concentration CO_2 and I_{fc}), respectively [38]. The open-circuit potential value of PEMFC dependent to temperature and gas pressure is expressed below [38,44]:

$$V_{oc} = K_c\left[V_o + (T-298)\frac{-44,43}{zF} + \frac{R_cT}{zF}\ln\left(\frac{P_{H_2}P_{O_2}^{1/2}}{P_{H_2O}}\right)\right] \tag{2}$$

where, K_c is a constant value in ($kmol/sA^{-1}$). In addition, T defines working temperature, R_c is the gas constant, F is

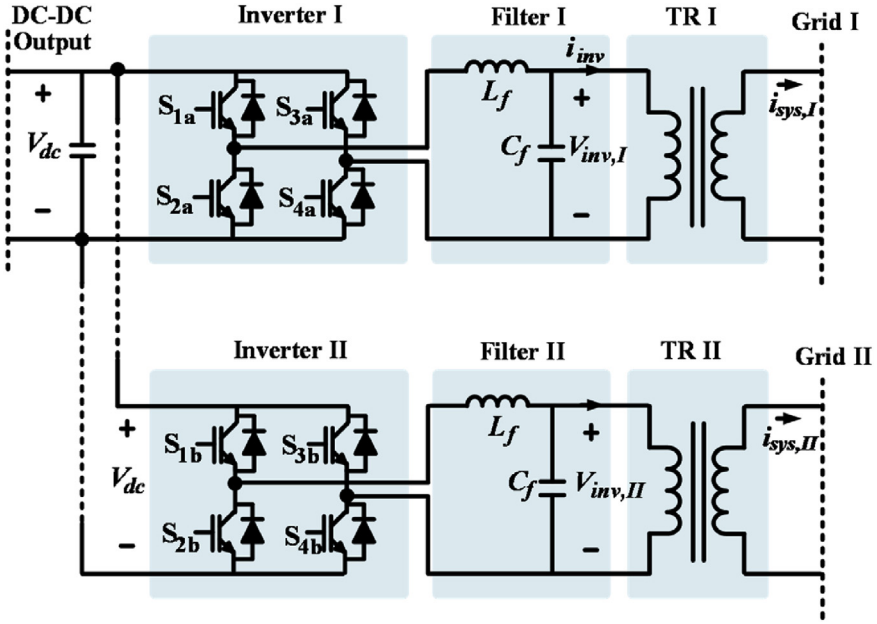

Fig. 4 – The connection of grid inverters in I-FC system.

Table 2 – The parameters and values of interface components between the fuel cell and grid.

Dc-dc Converter-side	
Type	Boost
Inductor (L)	0.6 mH
Dc-link capacitor (C)	10 mF
Reference	120 V
Inverter-side	
Type	H-bridge
Inverter I - Filter inductor & capacitor	0.3 mH, 20 uF
Inverter II - Filter inductor & capacitor	0.5 mH, 15 uF
Transformer I&II turn ratio (Np/Ns)	0.4

Faraday constant, P_{H_2} and P_{O_2} are the gas pressure values, V_o is an electromotive force for definitive pressure and z indicates the number of electrons moving. Ohmic overvoltage is defined dependent to fuel cell's current and structural resistance [26].

$$V_{ohmic} = i_{fc} R_{ohmic} \quad (3)$$

The absolute polarization overvoltage is described as:

$$v_d = N \times A \times \ln(i_{fc} / i_o) \quad (4)$$

N indicates the cell number in PEMFC. Besides, A and i_o define Tafel slope and exchange current detailed in Ref. [38]. The model of Ballard FCvelocity 9SSL PEMFC power generation unit used in the study is developed and validated based on the dynamic stack structure. The design parameters of Ballard FCvelocity 9SSL are given in Table 1.

Interfacing

In interfacing, dc-dc converters and inverters are the main elements between fuel cells and grids. Among these converters, the function of dc-dc converter in the grid connection of a PEMFC is to stabilize the voltage at the output of fuel cell and provide the efficient conversion for the input of inverter [51]. In this regard, the principal goal of dc-dc converter is to keep the inverter's input voltage fixed. In this study, boost topology is used to stabilize the voltage located between the fuel cell and grid inverters. In Fig. 3, the circuit scheme of a dc-dc boost converter is presented.

Table 3 – The specification of nonlinear loads connected to grid I and grid II.

Feeder I	
Grid Voltage	$220\sqrt{2}\mathrm{Sin}(2\pi 50t+0^\circ)$
Nonlinear load type	Uncontrolled rectifier
R1	4 Ω
C1	3 mF
R2	2.5 Ω
Feeder II	
Grid Voltage	$220\sqrt{2}\mathrm{Sin}(2\pi 50t+60^\circ)$
Nonlinear load type	Uncontrolled rectifier
R3	3 Ω
C2	0.2 mF
R4	5 Ω

In the dc-link control of boost converter, a PI controller is employed to generate reference signals for the switching process [52]. The PI controller takes the difference of actual voltage and the desired reference value to generate the required signal for triggering switch through pulse width modulation [53]. The dc-dc boost converter is operated in continuous mode and the switching time called duty cycle (*D*) determines the conversion ratio. The output voltage in boost converter is defined as:

$$V_{dc} = V_{fc}/(1-D) \quad (5)$$

where V_{dc} is output voltage, V_{fc} is fuel cell voltage and *D* is duty cycle.

In the output of a fuel cell, the power/voltage are produced in dc form. However, these systems must ensure power to the main grids in ac form [54]. For this reason, the structures are connected to the grids through inverters. In the proposed study, the generated power is supplied from the fuel cell to the different feeders through separate grid inverters. The power and voltage at the fuel cell output are generated in dc form, but they must be supplied to the electrical grid in AC form [10,51]. For this purpose, inverters convert the dc voltage to ac voltage in order to supply the electrical energy into the grid [45]. Fig. 4 introduces the separate inverters with output filters and the isolation transformer in I-FC system.

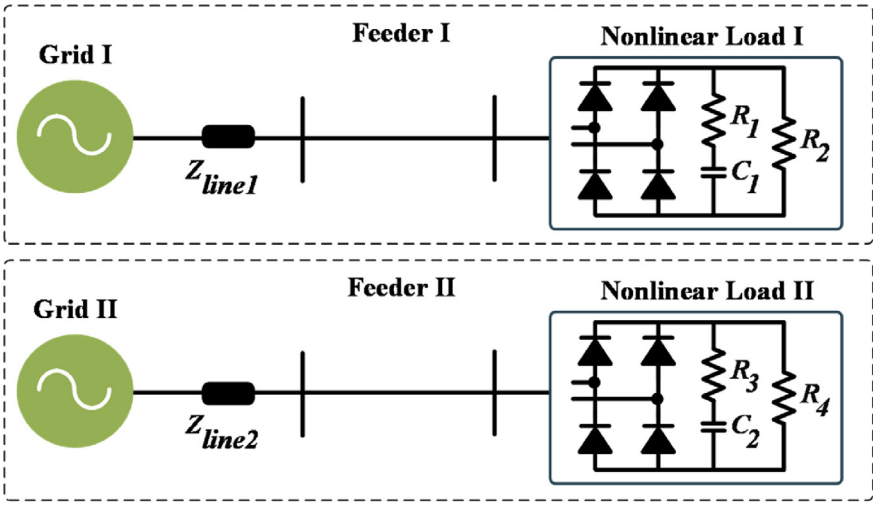

Fig. 5 – Grid connected nonlinear loads in the multi-feeder system.

The generated voltage at the output of H-bridge inverter is explained by using Fourier series. According to the Fourier series, the generated voltage includes merely odd harmonic parts in square-wave modulation technique [55]. The generated voltage by H-bridge inverter is written in Eqs. (6) and (7) [56]:

$$V_o(t) = \sum_{n=1}^{\infty} V_n \sin(n\omega_o t + \theta_n) \quad (6)$$

$$V_o(t) = \sum_{n-odd} \frac{4V_{dc}}{n\pi} \sin(n\omega_o t) \quad (7)$$

The fundamental control in I-FC system is achieved through separate inverters. However, they generate high-frequency noise signals in output voltages. For this purpose, LC filters are located at the outputs of parallel inverters for the elimination of switching ripples because of switching operation [57]. In addition, a step-up isolation transformer is located between grid-side inverter side [46,58]. The parameter and rating values of interfacing elements used in the I-FC system are presented in Table 2.

Grid with nonlinear loads

In the tested system, I-FC system is connected to multi-feeder electrical grids in the ratings of 220 Vrms/50 Hz. As shown in Fig. 5, full-bridge uncontrolled rectifiers are used as nonlinear loads in order to generate current harmonics which distort the power quality of grid currents [59]. Table 3 introduces the power ratings, impedance values and activation times of load banks.

I-FC control

The control steps for grid-inverters of I-FC system is introduced in Fig. 6. This controller is applied in the inverter parts of the I-FC system. The fundamental aims of the used method are to share active powers from the fuel cell to local loads and to reduce current harmonics in multi-feeder grids. Also, the detailed control mechanism of I-FC system is presented in Fig. 7. According to the controller mechanism, it consists of the four basic parts which are power control, current

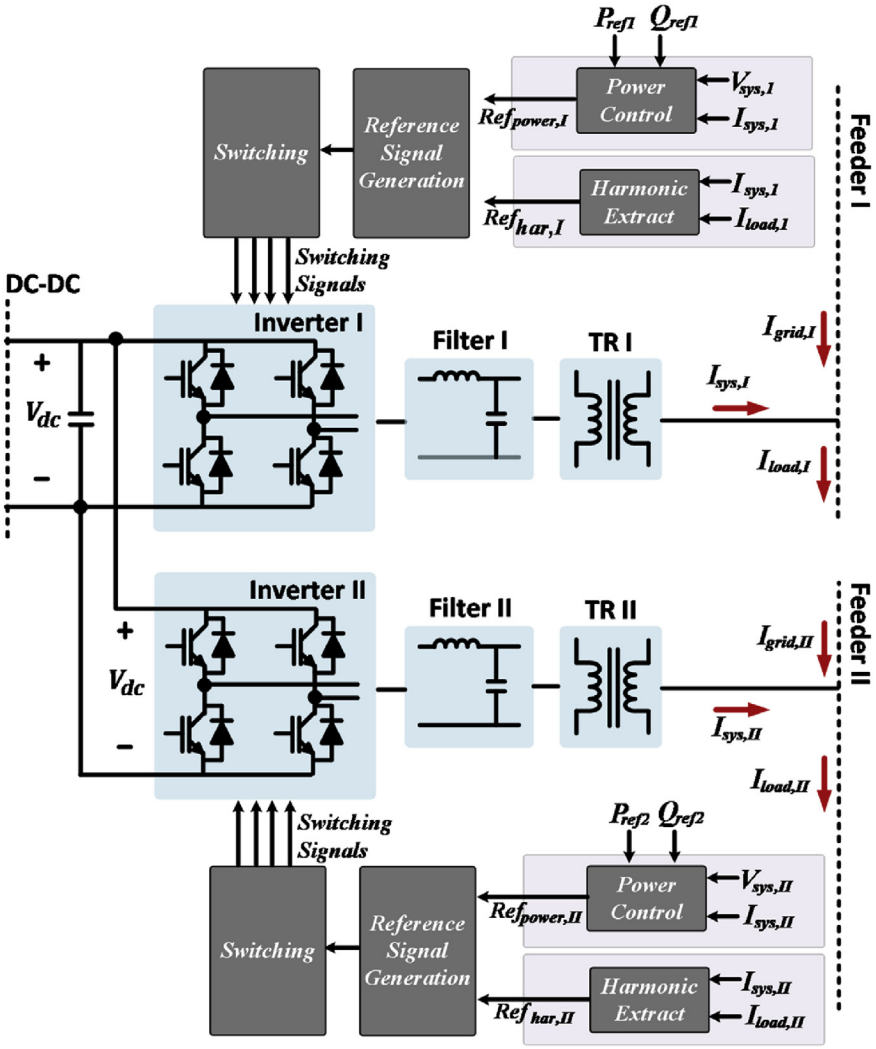

Fig. 6 – The control steps for grid inverters in I-FC system.

harmonic calculation, reference signal generation and switching process.

Power sharing

Inverter part is used to control the active/reactive power flow between the fuel cell and grid. In active power flow control, it is adjusted according to the fuel cell power rating. The real/reactive powers delivered by system I-part and system II-part are defined as $P_{sys,I}$ & $Q_{sys,I}$ and $P_{sys,II}$ & $Q_{sys,II}$. In I-FC system, the injected individual powers are the sum of supplied from the fuel cell. Therefore, the equations are defined as:

$$P_{total} = P_{sys,I} + P_{sys,II} \tag{8}$$

$$Q_{total} = Q_{sys,I} + Q_{sys,II} \tag{9}$$

In the proposed system, I-FC shares the supplied power into multi-feeders: feeder-I and feeder-II. The proposed system is designed to generate 18 kW power from fuel cells and to share it as 10 kW and 8 kW for feeder-I and feeder-II. However, the reactive power is not required to be transmitted to the system. For this purpose, the value of reactive power reference is adjusted to zero in order to provide zero reactive power flow between grid and inverters [28,45]. In this context, the actual voltages/currents at system-side are measured and used to calculate instantaneous power values. This is achieved by using αβ transformation according to Clarke's theory [45].

$$P_{sys,n} = \frac{1}{2}\left(V_{sys,n-\alpha} I_{sys,n-\alpha} + V_{sys,n-\beta} I_{sys,n-\beta}\right) \tag{10}$$

$$Q_{sys,n} = \frac{1}{2}\left(V_{sys,n-\beta} I_{sys,n-\alpha} - V_{sys,n-\alpha} I_{sys,n-\beta}\right) \tag{11}$$

In next step, the actual power magnitudes are transformed into dq frame [45]:

$$P_{sys,n} = \frac{3}{2}\left(V_{sys,n-d} i_{sys,n-d} + V_{sys,n-q} i_{sys,n-q}\right) \tag{12}$$

$$Q_{sys,n} = \frac{3}{2}\left(V_{sys,n-q} i_{sys,n-d} - V_{sys,n-d} i_{sys,n-q}\right) \tag{13}$$

In the grid side control, d-component is oriented in dq frame to control dc link voltage and power flow.

$$V_{sys,n-d} = V_{sys,n} \tag{14}$$

$$V_{sys,n-q} = 0 \tag{15}$$

According to the (14) and (15), the power equations are written in new form:

$$P_{sys,n} = \frac{3}{2} V_{sys,n-d} i_{sys,n-d} \tag{16}$$

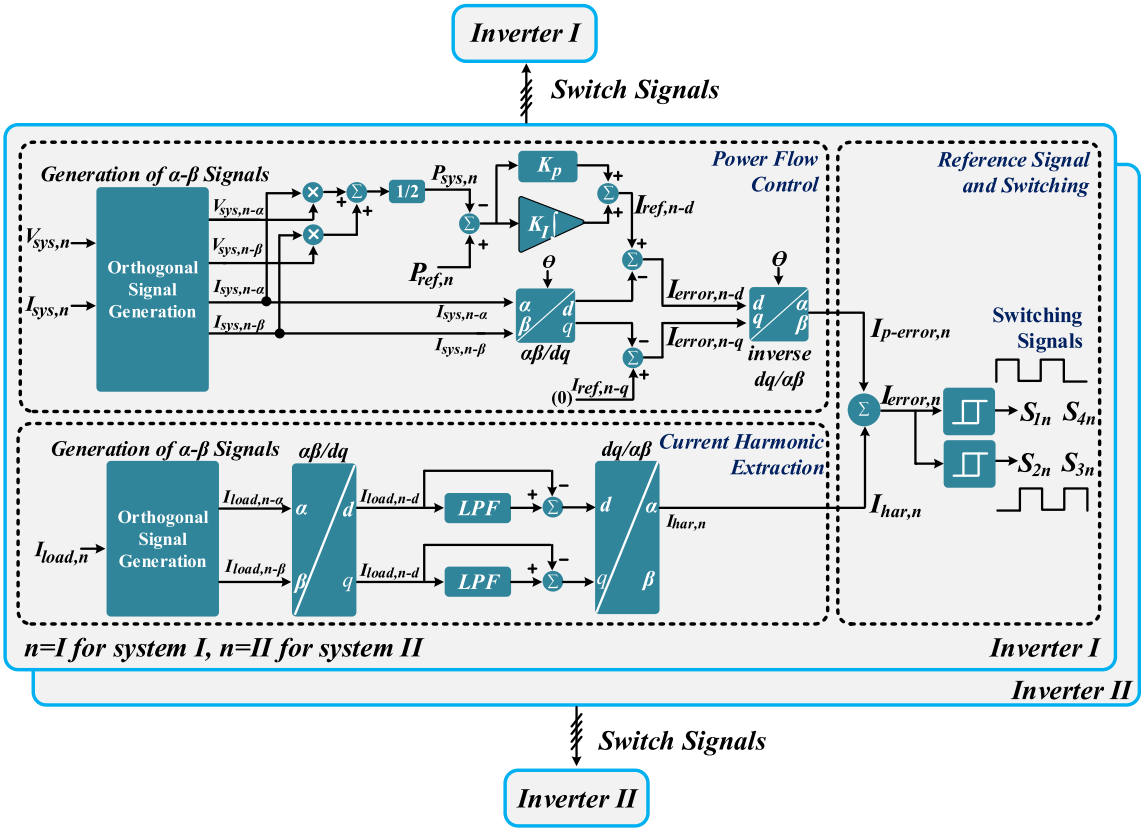

Fig. 7 – Dual functional control scheme of I-FC system.

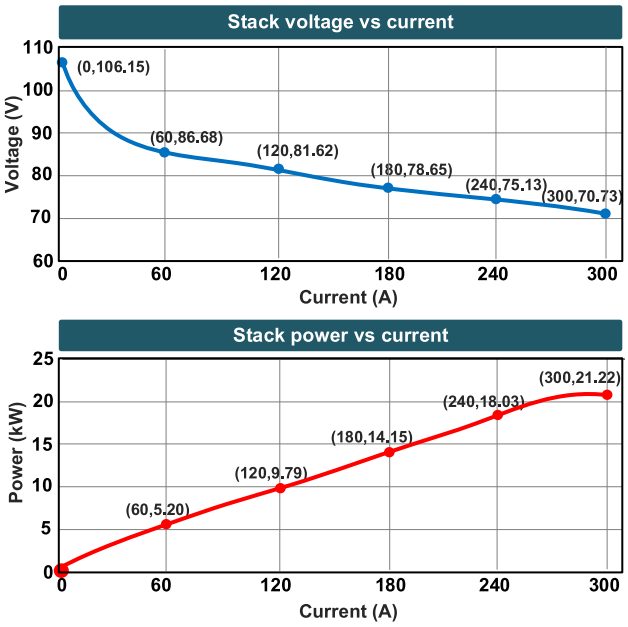

Fig. 8 – The characteristics of Ballard FC-velocity PEMFC stack.

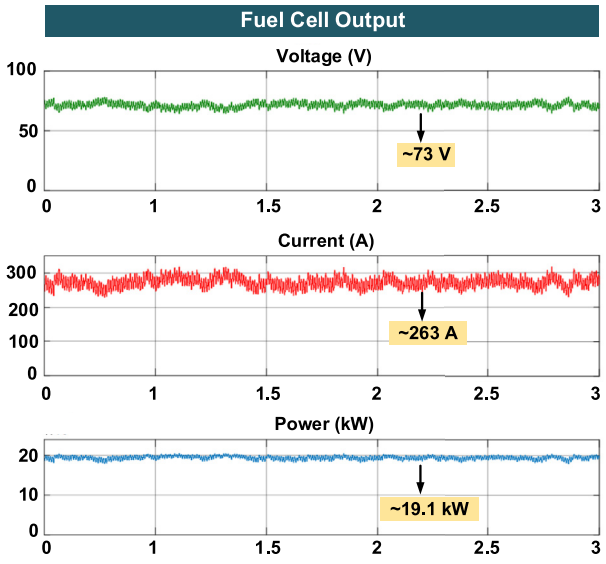

Fig. 9 – The electrical waveforms at fuel cell output.

$$Q_{sys,n} = -\frac{3}{2} V_{sys,n-d} i_{sys,n-q} \tag{17}$$

It is clear that the real power is controlled by using only d component of current, and q component of system current is applied in reactive power control between inverter and grid [28]. By using reference and actual values of active/reactive powers, d and q components are calculated through PI and P controller, respectively [44].

$$I_{ref,n-d} = K_p \left(P_{ref,n} - P_{sys,n}\right) + K_i \int \left(P_{ref,n} - P_{sys,n}\right) dt \tag{18}$$

$$I_{ref,n-q} = K_p \left(Q_{ref,n} - Q_{sys,n}\right) \tag{19}$$

where $P_{ref,n}$ is power sharing value for inverter I and II, respectively. $Q_{ref,n}$ is zero.

The actual d and q components of inverter currents are calculated by using $I_{sys,n}$. In this transform, orthogonal signals are used as inputs. By using α and β components, dq components are generated as below [45]:

$$\begin{bmatrix} I_{actual,n-d} \\ I_{actual,n-q} \end{bmatrix} = \begin{bmatrix} \cos(\omega t) & \sin(\omega t) \\ -\sin(\omega t) & \cos(\omega t) \end{bmatrix} \begin{bmatrix} I_{sys,n-\alpha} \\ I_{sys,n-\beta} \end{bmatrix} \tag{20}$$

$I_{actual,n-d}$ and $I_{actual,n-q}$ can be written as follows:

$$I_{actual,n-d} = I_{sys,n-\alpha} \cos(\omega t) + I_{sys,n-\beta} \sin(\omega t) \tag{21}$$

$$I_{actual,n-q} = -I_{sys,n-\alpha} \sin(\omega t) + I_{sys,n-\beta} \cos(\omega t) \tag{22}$$

By the subtraction of references and actual values, final currents are computed in dq reference frame. These equations are expressed as follows [28]:

$$I_{error,n-d} = I_{ref,n-d} - I_{actual,n-d} \tag{23}$$

$$I_{error,n-q} = I_{ref,n-q} - I_{actual,n-q} \tag{24}$$

In the inverse reference frame, the reference signal of power flow is converted from dq to $\alpha\beta$. In this transformation, α component gives the reference signal because of a single

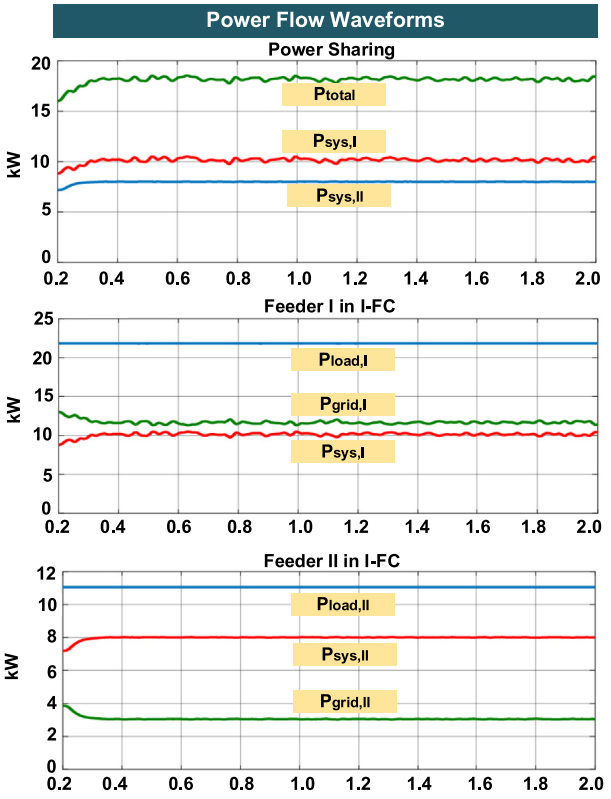

Fig. 10 – The power flow in I-FC connected grid system with local loads.

phase system. The inverse dq to αβ transform is realized in this form [60,61]:

$$\begin{bmatrix} I_\alpha \\ I_\beta \end{bmatrix} = \begin{bmatrix} \cos(\omega t) & -\sin(\omega t) \\ \sin(\omega t) & \cos(\omega t) \end{bmatrix} \begin{bmatrix} I_{error,n-d} \\ I_{error,n-q} \end{bmatrix} \quad (25)$$

By using inverse dq transform, the difference between actual and measured signals is defined as an error in the reference frame. In the controller, it is a single phase and only α-output is used as an error signal ($I_{p-error,n} = I_\alpha$). It is written as follows:

$$I_{p-error,n} = I_\alpha = I_{error,n-d}\cos(\omega t) - I_{error,n-q}\sin(\omega t) \quad (26)$$

Harmonic extraction

Current harmonics are extracted in the synchronous reference frame. For this purpose, the measured load currents are first transformed into α and β components. In next step, these components are converted to d and q components.

$$\begin{bmatrix} I_{load,n-d} \\ I_{load,n-q} \end{bmatrix} = \begin{bmatrix} \cos(\omega t) & -\sin(\omega t) \\ \sin(\omega t) & \cos(\omega t) \end{bmatrix} \begin{bmatrix} I_{error,n-\alpha} \\ I_{error,n-\beta} \end{bmatrix} \quad (27)$$

It is known that $I_{load,n-d}$ and $I_{load,n-q}$ consist of harmonic components in distorted current conditions. In dq frame, fundamental part is in dc form but harmonic components act as ac constituents [62]. The definitions of these components are given in:

$$I_{load,n-d} = \bar{I}_{load,n-d} + \tilde{I}_{load,n-d} \quad (28)$$

$$I_{load,n-q} = \bar{I}_{load,n-q} + \tilde{I}_{load,n-q} \quad (29)$$

where $\bar{I}_{load,n-d}$ and $\bar{I}_{load,n-q}$ are dc components, $\tilde{I}_{load,n-d}$ and $\tilde{I}_{load,n-q}$ are AC components. By using low-pass filters, Ĩload,n-d, Ĩload,n-q are extracted from $I_{load,n-d}$ and $I_{load,n-q}$. In continuation, harmonic components ($\tilde{I}_{load,n-d}$ and $\tilde{I}_{load,n-q}$) are converted to α-component by using inverse αβ-dq transform.

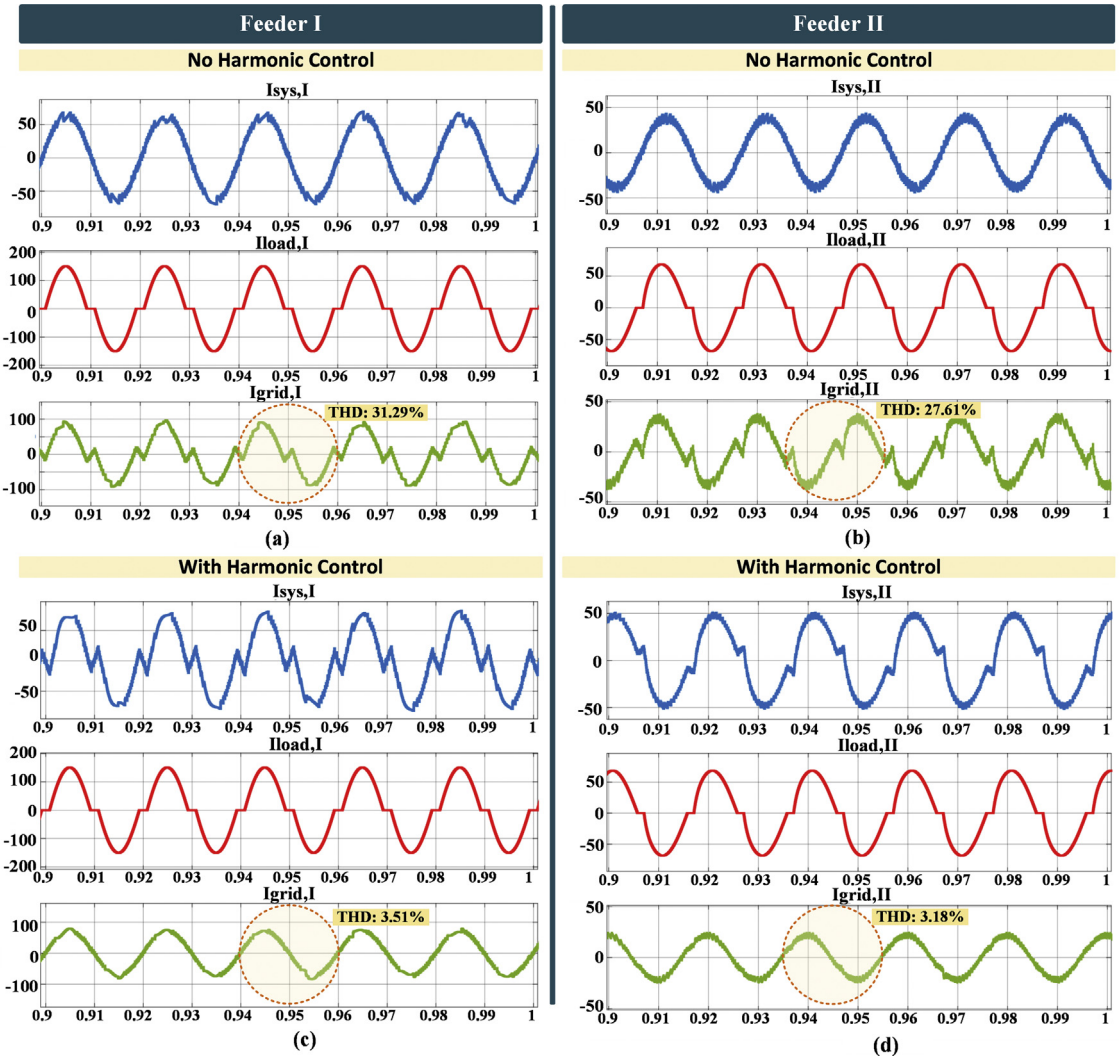

Fig. 11 – The current waveforms for (a) feeder I with no harmonic control, (b) feeder II with no harmonic control, (c) feeder I with harmonic elimination capability, and (d) feeder II with harmonic elimination capability.

$$[I_{har,n}] = [I_{\alpha}] = [\cos(\omega t)\ \sin(\omega t)] \begin{bmatrix} \tilde{I}_{load,n-d} \\ \tilde{I}_{load,n-q} \end{bmatrix} \quad (30)$$

$$I_{har,n} = \tilde{I}_{load,n-d}\cos(\omega t) + \tilde{I}_{load,n-q}\sin(\omega t) \quad (31)$$

Reference signal and switching

Reference signal in multifunctional compensation consists of harmonics and dip/swell components. The compensation of harmonics is achieved with injection of inverse voltage in addition to dip/swell compensation. Therefore, reference signal is the sum of $I_{p-error,n}$ and inverse of $I_{har,n}$.

$$I_{error,n} = I_{p-error,n} + I_{har,n} \quad (32)$$

In which, $I_{error,n}$ is used in switching process.

The obtained reference signal ($I_{error,n}$) is employed in the hysteresis pulse width modulation to generate switching signals for H-bridge inverters [63]. The upper and lower values of the hysteresis band are adjusted according to the inverter current. Switches are triggered according to the following hysteresis rule:

$$I_{error,n} > h \rightarrow S_{1,n}\&S_{4,n} \quad (33)$$

$$I_{error,n} < h \rightarrow S_{2,n}\&S_{3,n} \quad (34)$$

In which, h defines the hysteresis band. Also, it is selected as 0.02 in the proposed system.

Performance results

In this work, I-FC system is designed and tested by using 19.2 kW Ballard FC-velocity PEMFC stack. The designed system has been performed to protect multi-feeders against current harmonics and share active powers supplied from PEMFC to grids. For this purpose, nonlinear loads are connected to grids in order to create harmonic distortions in the ratings of 31.19% and 27.23%, respectively. By this way, the model has been constructed and tested via Simulink environment program. In order to analyze the grid-connected I-FC system, grid voltages are selected as 220 Vrms/50 Hz in 0-degree and 60-degree reference phase angles. The voltage and power characteristics curve of Ballard FC-velocity PEMFC stack are given in Fig. 8 according to the operating conditions. In nominal operating conditions, it is adjusted to generate approximately 18 kW power at output.

The electrical characteristics of the fuel cell during the operation state is introduced in Fig. 9. The waveforms show that the fuel cell voltage/current are equal to approximately 73 V and 263 A, respectively. The power supplied from fuel cell to grids is equal to nominal power 19.2 kW.

The grid-connected I-FC system is used to share supplied power and mitigate the current harmonics at grid-side currents. Fig. 10 presents the power waveforms in I-FC connected multi-feeder. In Fig. 10, it shows the power-sharing values for part I and part II of I-FC. P_{total} is the value

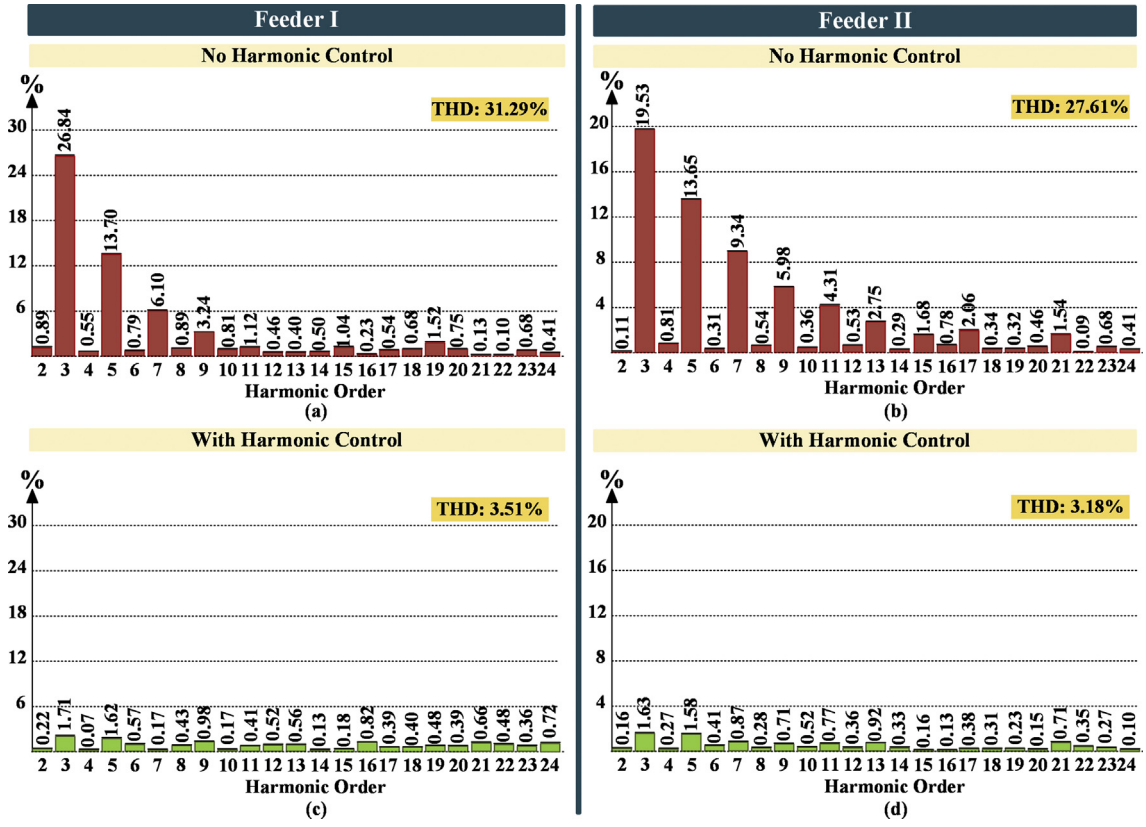

Fig. 12 – THD spectrum for current harmonics (a) feeder I with no harmonic control, (b) feeder II with no harmonic control, (c) feeder I with harmonic elimination capability, and (d) feeder II with harmonic elimination capability.

supplied from the fuel cell and is equal to the sum of $P_{sys,I}$ and $P_{sys,II}$. In feeder I, the system I supply 10 kW into the feeder I. But, the nonlinear load consumes 22.1 kW and ensure the 12.1 kW from the grid. While I-FC provides 8 kW for the system-II, nonlinear load II demands 10.9 kW in the steady-state. Therefore, it absorbs the remainder part from the grid-side.

In addition to the power supply by I-FC system, it can also attenuate the current harmonics due to nonlinear loads connected in feeder I and feeder II, as shown in Fig. 11. Among these loads, load I causes a harmonic distortion which its value is equal to 31.29% THD at grid-current. After the operation by I-FC with enabling the current harmonic elimination capability, the THD value at grid current reduces to 3.51% which is satisfied by IEEE-519 Std. 1993. When the power flow control capability is active without harmonic mitigation capability, THD value for grid-current at feeder II is 27.61% due to the load II. It should be noted that THD value drops to 3.18% after the harmonic elimination capability by I-FC system.

As presented in Fig. 12, FFT spectrum for grid-side current is given up to 25th harmonics. It is obvious that 3rd, 5th and 7th harmonics are the most considerable components which are greater than 5%. By the elimination with I-FC system, these components appear to be significantly reduced. The results show the harmonic orders up to 25th components.

Conclusion

In this work, a new approach in the grid-connected fuel cell system is developed and tested for two-feeder system. In the presented configuration approach, the tested system shares a common dc-dc converter with fuel cell and it is named as Interline Fuel Cell (I-FC) system. In comparison with a conventional systems, it aims an economical way to mitigate the current harmonic problems at grid-side for multi-feeders. Also, this system uses a common dc-dc converter/fuel cell with different grid inverters and achieves:

- To control power-sharing between lines and
- To mitigate the harmonic problems at grid-side currents.

For this purpose, a dual functional controller based on αβ-dq transform is performed in the grid inverters, separately. By using the controller, the reference signals of injected powers & current harmonics are obtained, respectively. The final reference signal which consists of power reference and current harmonics is separately used in the switching process for grid inverters. In the design process, the dynamic model of Ballard FCvelocity 9SSL is used in the I-FC system for a generation the required active power supplied to electrical feeders. Also, it is connected to grid-inverters through a dc-dc boost converter. The designed system achieves the power-sharing in the ratings of 10 kW and 8 kW for feeder I and feeder II. Also, the current harmonics due to nonlinear loads are significantly reduced to values less than 5% THD, which is defined by IEEE-519 standards. In order to show the differences before/after the harmonic elimination capability, THD spectrums of grid currents are presented for feeder I and feeder II.

REFERENCES

[1] İnci M, Türksoy Ö. Review of fuel cells to grid interface: configurations, technical challenges and trends. J Clean Prod 2019;213:1353–70.

[2] Mehrjerdi H. Off-grid solar powered charging station for electric and hydrogen vehicles including fuel cell and hydrogen storage. Int J Hydrogen Energy 2019;44(23):11574–83.

[3] Attemene N, Agbli KS, Fofana S, Hissel D. Optimal sizing of a wind, fuel cell, electrolyzer, battery and supercapacitor system for off-grid applications. Int J Hydrogen Energy 2019. https://doi.org/10.1016/j.ijhydene.2019.05.212.

[4] Bornapour M, Hooshmand RA, Khodabakhshian A, Parastegari M. Optimal coordinated scheduling of combined heat and power fuel cell, wind, and photovoltaic units in micro grids considering uncertainties. Energy 2016;117:176–89.

[5] Lu YZ, Cai YX, Souamy L, Song X, Zhang L, Wang J. Solid oxide fuel cell technology for sustainable development in China: an over-view. Int J Hydrogen Energy 2018;43(28):12870–91.

[6] Argyrou MC, Christodoulides P, Kalogirou SA. Energy storage for electricity generation and related processes: technologies appraisal and grid scale applications. Renew Sustain Energy Rev 2018;94:804–21.

[7] Yu S, Fernando T, Chau TK, Iu HH. Voltage control strategies for solid oxide fuel cell energy system connected to complex power grids using dynamic state estimation and STATCOM. IEEE Trans Power Syst 2017;32(4):3136–45.

[8] Maleki A, Hafeznia H, Rosen MA, Pourfayaz F. Optimization of a grid-connected hybrid solar-wind-hydrogen CHP system for residential applications by efficient metaheuristic approaches. Appl Therm Eng 2017;123:1263–77.

[9] Ali ES, Abd Elazim SM, Abdelaziz AY. Optimal allocation and sizing of renewable distributed generation using ant lion optimization algorithm. Electr Eng 2018;100(1):99–109.

[10] Sharma RK, Mishra S. Dynamic power management and control of a PV PEM fuel-cell-based standalone ac/dc microgrid using hybrid energy storage. IEEE Trans Ind Appl 2018;54(1):526–38.

[11] Trujillo Caballero JC, Roffiel JA, López Mariño MA, Morgado Lievana OR, Pouresmaeil E, Vechiu I. A control method for operation of a power conditioner system based on fuel cell/supercapacitor. Electr Eng 2018;100(2):857–63.

[12] Cossutta P, Aguirre MP, Cao A, Raffo S, Valla MI. Single-stage fuel cell to grid interface with multilevel current-source inverters. IEEE Trans Ind Electron 2015;62(8):5256–64.

[13] Sergi F, Brunaccini G, Stassi A, Di Blasi A, Dispenza G, Arico AS, Ferraro M, Antonucci V. PEM fuel cells analysis for grid connected applications. Int J Hydrogen Energy 2011;36(17):10908–16.

[14] Gharibi M, Askarzadeh A. Size and power exchange optimization of a grid-connected diesel generator-photovoltaic-fuel cell hybrid energy system considering reliability, cost and renewability. Int J Hydrogen Energy 2019.

[15] Mosaad MI, Ramadan HS. Power quality enhancement of grid-connected fuel cell using evolutionary computing techniques. Int J Hydrogen Energy 2018;43(25):11568–82.

[16] Han B, Bai C, Lee JS, Kim M. Repetitive controller of capacitor-less current-fed dual-half-bridge converter for grid-connected fuel cell system. IEEE Trans Ind Electron 2018;65(10):7841–55.
[17] Bayrak G, Cebeci M. A novel anti islanding detection method for grid connected fuel cell power generation systems. Int J Hydrogen Energy 2014;39(16):8872–80.
[18] Sekhar PC, Mishra S. Sliding mode based feedback linearizing controller for grid connected multiple fuel cells scenario. Int J Elec Power 2014;60:190–202.
[19] Zhang LF, Xiang J. The performance of a grid-tied microgrid with hydrogen storage and a hydrogen fuel cell stack. Energy Convers Manag 2014;87:421–7.
[20] El-Sharkh MY, Tanrioven M, Rahman A, Alam MS. A study of cost-optimized operation of a grid-parallel PEM fuel cell power plant. IEEE Trans Power Syst 2006;21(3):1104–14.
[21] Li YH, Rajakaruna S, Choi SS. Control of a solid oxide fuel cell power plant in a grid-connected system. IEEE Trans Energy Convers 2007;22(2):405–13.
[22] Marquezini DD, Ramos DB, Machado RQ, Farret FA. Interaction between proton exchange membrane fuel cells and power converters for AC integration. IET Renew Power Gener 2008;2(3):151–61.
[23] Mazumder SK, Burra RK, Huang RJ, Tahir M, Acharya K. A universal grid-connected fuel-cell inverter for residential application. IEEE Trans Ind Electron 2010;57(10):3431–47.
[24] Li WH, Li WC, Deng Y, He XN. Single-stage single-phase high-step-up ZVT boost converter for fuel-cell microgrid system. IEEE Trans Power Electron 2010;25(12):3057–65.
[25] Ayyappa SK, Gaonkar DN. Performance analysis of a variable-speed wind and fuel cell-based hybrid distributed generation system in grid-connected mode of operation. Electr Power Compon Syst 2016;44(2):142–51.
[26] Li Q, Chen WR, Liu ZX, Zhou GH, Ma L. Active control strategy based on vector-proportion integration controller for proton exchange membrane fuel cell grid-connected system. IET Renew Power Gener 2015;9(8):991–9.
[27] Du W, Wang HF, Zhang XF, Xiao LY. Effect of grid-connected solid oxide fuel cell power generation on power systems small-signal stability. IET Renew Power Gener 2012;6(1):24–37.
[28] Jang M, Ciobotaru M, Agelidis VG. A single-phase grid-connected fuel cell system based on a boost-inverter. IEEE Trans Power Electron 2013;28(1):279–88.
[29] Ghazanfari A, Hamzeh M, Mokhtari H, Karimi H. Active power management of multihybrid fuel cell/supercapacitor power conversion system in a medium voltage microgrid. IEEE Trans Smart Grid 2012;3(4):1903–10.
[30] Reznik A, Simoes MG, Al-Durra A, Muyeen SM. LCL filter design and performance analysis for grid-interconnected systems. IEEE Trans Ind Appl 2014;50(2):1225–32.
[31] Sun L, Jin Y, Pan L, Shen J, Lee KY. Efficiency analysis and control of a grid-connected PEM fuel cell in distributed generation. Energy Convers Manag 2019;195:587–96.
[32] Erfanmanesh T, Dehghani M. Performance improvement in grid-connected fuel cell power plant: an LPV robust control approach. Int J Electr Power Energy Syst 2015;67:306–14.
[33] Padmanaban S, Priyadarshi N, Bhaskar MS, Holm-Nielsen JB, Hossain E, Azam F. A hybrid photovoltaic-fuel cell for grid integration with jaya-based maximum power point tracking: experimental performance evaluation. IEEE Access 2019;7:82978–90.
[34] Roy AK, Basak P, Biswal GR. Low voltage ride through capability enhancement in a grid-connected wind/fuel cell hybrid system via combined feed-forward and fuzzy logic control. IET Gener Transm Distrib 2019;vol. 13(13):2866–76.
[35] Buyuk M, Inci M, Tumay M. Performance evaluation of LLCL filter for active power filter. In: 2016 IEEE 16th international conference on environment and electrical engineering (EEEIC); 2016. p. 1–4.
[36] IEEE recommended practice and requirements for harmonic control in electric power systems. In: IEEE Std 519-2014 (Revision of IEEE Std 519-1992); 2014. p. 1–29.
[37] Auld AE, Brouwer J, Smedley KM, Samuelsen S. Load-following strategies for evolution of solid oxide fuel cells into model citizens of the grid. IEEE Trans Energy Conver 2009;24(3):617–25.
[38] Chen WR, Han Y, Li Q, Liu ZX, Peng F. Design of proton exchange membrane fuel cell grid-connected system based on resonant current controller. Int J Hydrogen Energy 2014;39(26):14402–10.
[39] Lee JG, Choe SY, Ahn JW, Baek SH. Modelling and simulation of a polymer electrolyte membrane fuel cell system with a PWM DC/DC converter for stationary applications. IET Power Electron 2008;1(3):305–17.
[40] Naik R, Mohan N, Rogers M, Bulawka A. A novel grid interface, optimized for utility-scale Applications of photovoltaic, wind-electric, and fuel-cell systems. IEEE T Power Deliver 1995;10(4):1920–6.
[41] Tan KT, So PL, Chu YC, Chen MZQ. Coordinated control and energy management of distributed generation inverters in a microgrid. IEEE T Power Deliver 2013;28(2):704–13.
[42] Tejwani V, Suthar B. Power management in fuel cell based hybrid systems. Int J Hydrogen Energy 2017;42(22):14980–9.
[43] Das D, Haque ME, Gargoom A, Muoka PI, Negnevitsky M. Operation and control of grid integrated hybrid wind-fuel cell system with STATCOM. Austr Univ Power Eng; 2012.
[44] Hajizadeh A, Golkar MA, Feliachi A. Voltage control and active power management of hybrid fuel-cell/energy-storage power conversion system under unbalanced voltage sag conditions. IEEE Trans Energy Convers 2010;25(4):1195–208.
[45] Mojallal A, Lotfifard S. Improving during and postfault response of fuel cells in symmetrical and asymmetrical grid fault cases. IEEE Trans Sustain Energy 2018;9(3):1407–18.
[46] Stewart EM, Tumilty R, Fletcher J, Lutz A, Ault G, McDonald J. Analysis of a distributed grid-connected fuel cell during fault conditions. IEEE Trans Power Syst 2010;25(1):497–505.
[47] Çelík D, Meral ME. A flexible control strategy with overcurrent limitation in distributed generation systems. Int J Electr Power Energy Syst 2019;104:456–71.
[48] Çelik D, Meral ME. A novel control strategy for grid connected distributed generation system to maximize power delivery capability. Energy 2019;186:115850.
[49] Alegria E, Brown T, Minear E, Lasseter RH. CERTS microgrid demonstration with large-scale energy storage and renewable generation. IEEE T Smart Grid 2014;5(2):937–43.
[50] Liso V, Nielsen MP, Kaer SK, Mortensen HH. Thermal modeling and temperature control of a PEM fuel cell system for forklift applications. Int J Hydrogen Energy 2014;39(16):8410–20.
[51] Mohr M, Franke WT, Wittig B, Fuchs FW. Converter systems for fuel cells in the medium power range-A comparative study. IEEE Trans Ind Electron 2010;57(6):2024–32.
[52] Meral ME, Celik D. Comparison of SRF/PI- and STRF/PR-based power controllers for grid-tied distributed generation systems. Electr Eng 2018;100(2):633–43.
[53] Raoufat ME, Khayatian A, Mojallal A. Performance recovery of voltage source converters with application to grid-connected fuel cell DGs. IEEE Trans Smart Grid 2018;9(2):1197–204.
[54] Thale SS, Wandhare RG, Agarwal V. A novel reconfigurable microgrid architecture with renewable energy sources and storage. IEEE Trans Ind Appl 2015;51(2):1805–16.

[55] Tommaso AOD, Livreri P, Miceli R, Schettino G, Viola F. A novel method for harmonic mitigation for single-phase five-level cascaded H-Bridge inverter. In: 2018 thirteenth international conference on ecological vehicles and renewable energies (EVER); 2018. p. 1–7.
[56] Aboadla EHE, Khan S, Habaebi MH, Gunawan T, Hamidah BA, Tohtayong M. Modulation optimization effect on total harmonic distortion of single phase H-bridge inverter based selective harmonics elimination technique. In: 2016 international conference on computer and communication engineering (ICCCE); 2016. p. 200–3.
[57] Buyuk M, Tan A, Tumay M, Bayindir KC. Topologies, generalized designs, passive and active damping methods of switching ripple filters for voltage source inverter: a comprehensive review. Renew Sustain Energy Rev 2016;62:46–69.
[58] Giustiniani A, Petrone G, Spagnuolo G, Vitelli M. Low-frequency current oscillations and maximum power point tracking in grid-connected fuel-cell-based systems. IEEE Trans Ind Electron 2010;57(6):2042–53.
[59] Yao Z, Xiao L. Control of single-phase grid-connected inverters with nonlinear loads. IEEE Trans Ind Electron 2013;60(4):1384–9.
[60] Emanuel AE, Milanez DL. Clarke's alpha, beta, and zero components: a possible approach for the conceptual design of instrumentation compatible with IEEE Std. 1459–2000. IEEE Trans Instrum Meas 2006;55(6):2088–95.
[61] Arboleya P, Gonzalez-Moran C, Coto M. Unbalanced power flow in distribution systems with embedded transformers using the complex theory in alpha beta 0 stationary reference frame. IEEE Trans Power Syst 2014;29(3):1012–22.
[62] Tan A, Bayındır KÇ, Cuma MU, Tümay M. Multiple harmonic elimination-based feedback controller for shunt hybrid active power filter. IET Power Electron 2017;10(8):945–56.
[63] Peter J, Shafi MKP, Lakshmi R, Ramchand R. Nearly constant switching space vector based hysteresis controller for VSI fed IM drive. IEEE Trans Ind Appl 2018;54(4):3360–71.